

Experimental investigation of 20 K two-stage layered active magnetic regenerative refrigerator

Inmyong Park, Sangkwon Jeong

Department of Mechanical Engineering, Korea Advanced Institute of Science and Technology, 373-1, Guseong-dong, Yuseong-gu, Daejeon 305-701, Korea

E-mail: impark@kaist.ac.kr

Abstract. The performance of a two-stage layered AMRR is experimentally investigated. The test apparatus includes two-stage layered AMRs, low temperature superconducting (LTS) magnet which generates maximum magnetic field of 4 T, and the helium gas flow system. The helium compressor with the tandem rotary valve is employed to generate the oscillating flow of the helium gas minimizing the pressure swing effect. The mass flow rate of working fluid is controlled separately at the first and second stages of the AMR by solenoid valves. The mass flow rate of the AMRs is measured by the mass flow meter and the cryogenic hot-film sensor which is calibrated at cryogenic temperature range from 20 K to 77 K. In order to reduce the heat leak by shuttle heat transfer of the working fluid, void volumes have been implemented and connected to the cold ends of the AMR1 and AMR2. The temperature span of the AMR is recorded as 52 K and the performance of the AMR with the variation of the mass flow rate is analysed. The results show that the mass flow rate and the heat leak due to the shuttle heat transfer by oscillating working fluid are crucial factors in the AMR performance.

1. Introduction

Magnetic refrigeration is one of the promising technologies to improve the efficiency of hydrogen liquefaction. A magnetic refrigerator utilizes magneto-caloric effect (MCE) of a magnetic refrigerant for cooling. Since MCE is a reversible process, it facilitates high thermodynamic efficiency of a magnetic refrigerator. An adiabatic demagnetization refrigerator (ADR), a type of magnetic refrigerator, has been used to obtain temperatures below 1 K by taking advantage of its inherent high thermodynamic efficiency [1-3]. However, the temperature span of an ADR is limited to a few degrees because the MCE only appears significantly near a magnetic ordering temperature. In contrast, an active magnetic regenerative refrigerator (AMRR), which is considered as the multi-stage cascade micro ADRs, can be employed to achieve low temperature even though the cold end temperature is significantly apart from the warm end temperature [4]. Because of its advantages, many previous researchers have focused on developing an AMRR with broad working temperature span. While enormous amount of room temperature AMRRs have been developed over the past several decades [5-9], a number of AMRRs for hydrogen liquefaction have been introduced over the past three decades [10-16]. Moreover, only half of them have been experimentally investigated [14-16].

In order to achieve a wide temperature span of an active magnetic regenerator (AMR), large magnetic entropy change over broad temperature range is required [4]. Because the MCE of a specific magnetic refrigerant occurs at limited temperature range near each refrigerant's magnetic ordering



temperature, multi-layered structure of the AMR with different kinds of magnetic refrigerants is indispensable. For instance, Numazawa et al. proposed multi-layered AMR with Fe-modified gadolinium gallium garnets (GGIG), HoAl_2 , and DyAl_2 in order to operate the AMR system between liquid nitrogen and liquid hydrogen temperature [14]. However, their experiment was limited to the single layered AMR. Kim et al. have described the layered AMR with four kinds of magnetic refrigerants [16]. The cold end of the AMR reached the lowest no-load temperature of 24 K and the temperature span was approximately 56 K. However, since the layered AMR system has some inherent cooling effect by gas expansion at the void volume under considerable pressure swing, each contribution from MCE and gas expansion on the overall cooling performance cannot be decoupled. Moreover, the exact mass flow rate of the working fluid in the layered AMR was unknown so that the experimental results cannot be compared to numerical results. Park et al. point out that the mass flow rate of the working fluid in the AMR is one of the key parameters which determines the performance of the AMRR [13].

This paper describes the modified version of the layered AMRR mentioned in the research of Kim et al. [16]. Design changes with respect to the previous experimental apparatus are illustrated in detail. The modified version of the layered AMRR system includes the tandem rotary valve, the hot-film sensor and the void volume. The experimental results of the modified AMRR system are extensively presented and analysed in this paper.

2. Experimental setup

The experimental apparatus in this paper consists of three main components: the helium gas flow

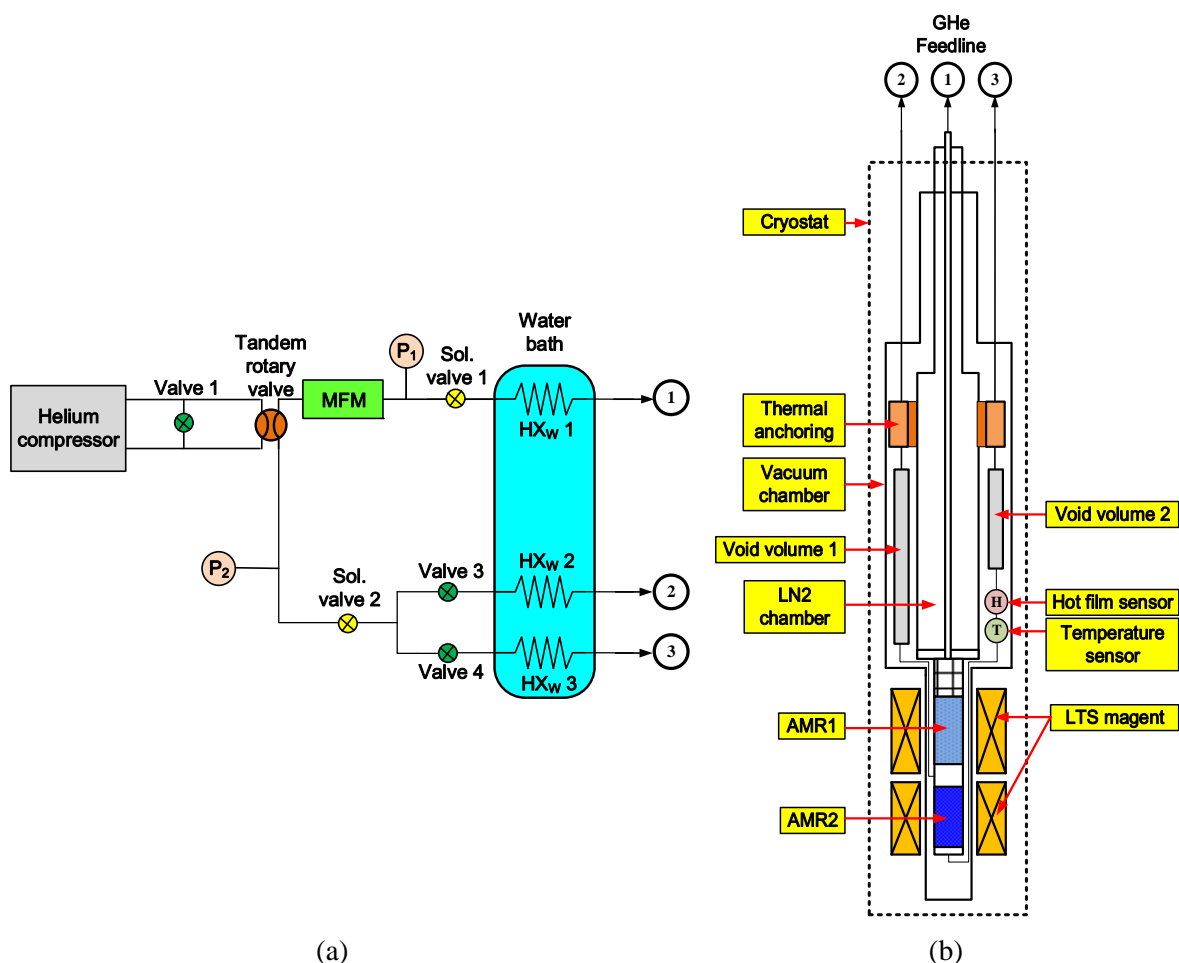


Figure 1. Schematic diagram of (a) the helium gas flow system and the experimental apparatus installed in the cryostat.

system, the AMR and the low temperature superconducting magnet. Figure 1 illustrates the schematic of the overall AMR system. The AMR system is based on the original one in that the basic configuration has remained same [16]. However, modification of the original AMR system has been conducted with the following considerations:

- 1) Minimization of the pulse tube effect caused by the buffer volume (pulse tubes and reservoir) under pressure swing
- 2) Measurement and control of the mass flow rate
- 3) Minimization of the shuttle heat transfer due to helium gas oscillation

1.1. Helium gas flow system

The previous version of the AMR system was constructed as a pulse tube configuration to generate oscillating flow of the helium gas into AMR. With the pulse tube refrigerator like configuration, the AMR system had some additional cooling effect by gas expansion at the pulse tubes. In order to eliminate the pulse tube effect, the pulse tubes and reservoir were removed and the tandem rotary valve with the solenoid valves have been installed to create oscillating flow with minimum pressure swing.

The tandem rotary valve has four ports. Two of them are connected to suction and discharge ports of the helium compressor (M125, Austin Scientific) and the others are linked to both ends of the AMR. When the helium compressor and the tandem rotary valve is in operation, suction and discharge ports of the helium compressor are alternatively connected to both ends of the AMR by the tandem rotary valve. As a result, the pressure alternation of the AMR generates oscillating flow of the helium gas. In addition to the tandem rotary valve, the solenoid valves are employed to control the mass flow rate. When the tandem rotary valve changes the direction of the gas flow, the solenoid valves which are connected to both ends of the AMR can open and close the passage of the gas flow according to the voltage signal from the control computer.

The mass flow rate of the AMR is measured by the mass flow meter and the hot film sensor

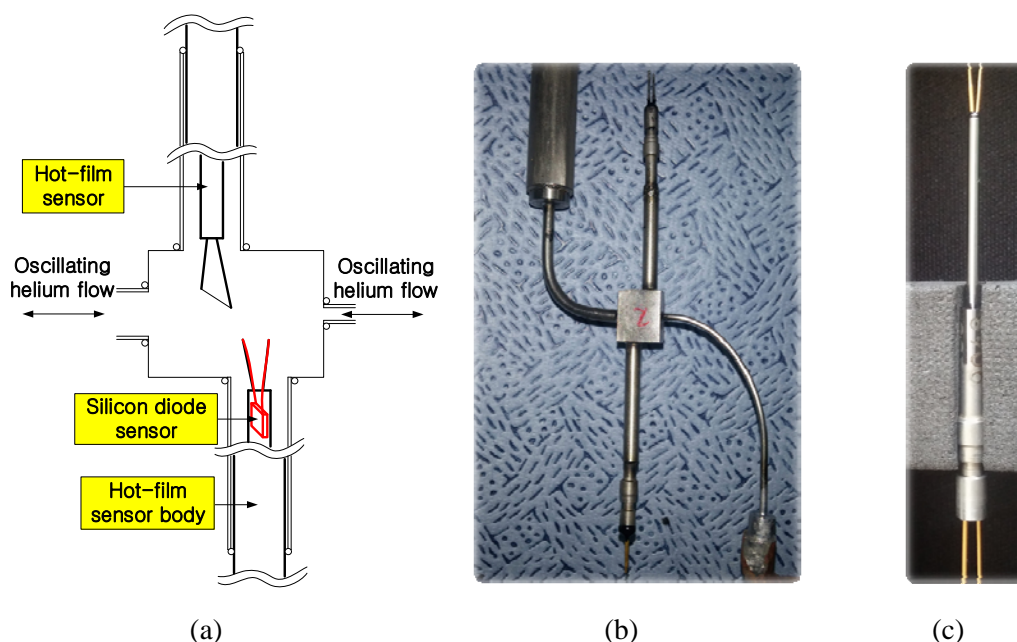


Figure 2. (a) Schematic diagram and (b) photo of the hot-film sensor assembly, and (c) photo of the hot-film.

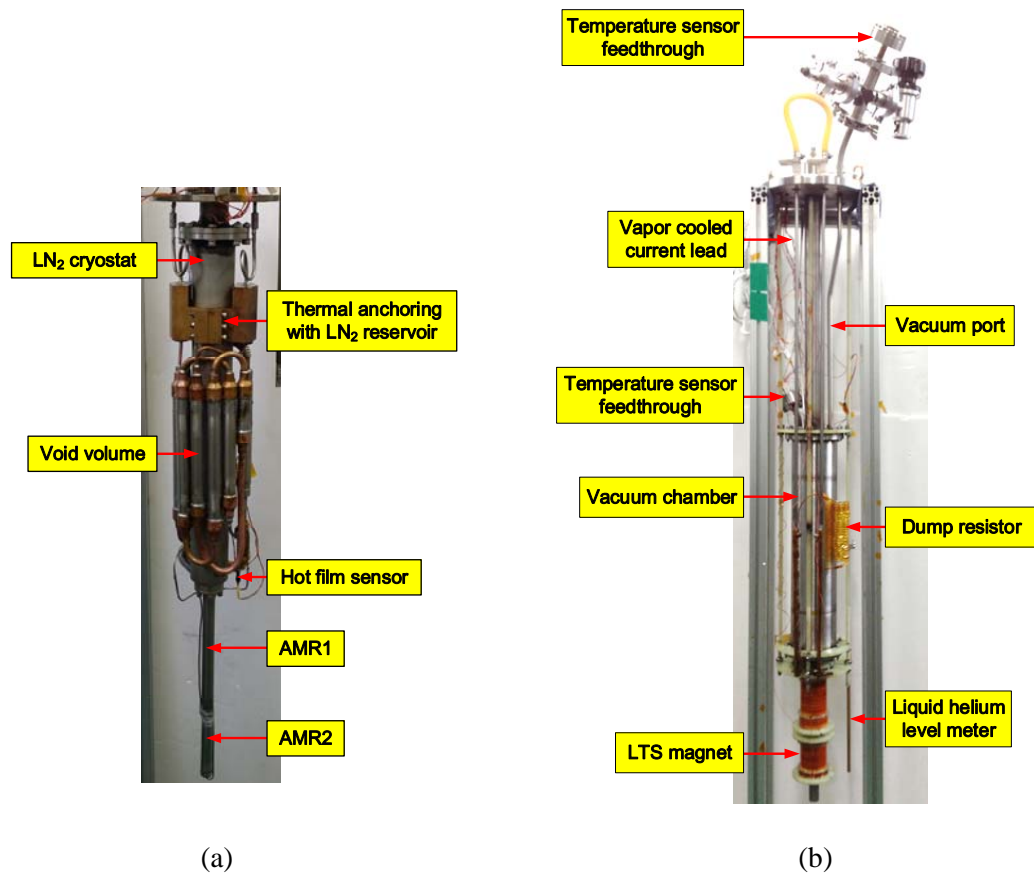


Figure 3. Photo of the experimental apparatus: (a) inside of the vacuum chamber, (b) outside of the vacuum chamber.

assembly which consists of the hot film sensor (1260A-10, TSI) and the temperature sensor (DT-670-SD, Lakeshore). Figure 2 shows the hot film sensor and its assembly. The hot film sensor assembly is connected to the cold end of the AMR2 illustrated in Fig. 1(b). The hot film sensor is carefully calibrated at the temperature between 20 K and 80 K.

Since the cooling effect of the pulse tubes at the cold-end of the AMR is minimized, the heat penetration caused by shuttle heat transfer of the helium gas has to be considered to improve the performance of the AMR. For instance, if there is any void volume between the thermal anchoring part with the LN₂ reservoir and the cold end of the AMR as shown in Fig. 3(a), the oscillation flow of the helium gas will directly transfer heat from the thermal anchoring to the cold end of the AMR. For this reason, we need ample void volumes between the thermal anchoring and the cold end of the AMR. The void volumes in this paper are made by 1/2 inch thin-walled stainless steel tubes and copper sockets. The configuration of the void volumes are quite complicated due to lack of the space in the vacuum chamber which separates the AMR and liquid helium. The total volumes of the void volume1 and the void volume2 are calculated as $8 \times 10^{-5} \text{ m}^3$ and $5 \times 10^{-5} \text{ m}^3$, respectively. The detailed AMR system inside of the cryostat is shown Fig.3.

1.2. AMR and superconducting magnet

The multi-layered AMR and the superconducting magnet in the previous research [16] are used in this experimental investigation. Four rare-earth based intermetallic compounds (GdNi_2 , $\text{Dy}_{0.85}\text{Er}_{0.15}\text{Al}_2$, $\text{Gd}_{0.1}\text{Dy}_{0.9}\text{Ni}_2$, $\text{Dy}_{0.5}\text{Er}_{0.5}\text{Al}_2$) are selected as the magnetic refrigerants. GdNi_2 and $\text{Dy}_{0.85}\text{Er}_{0.15}\text{Al}_2$ are

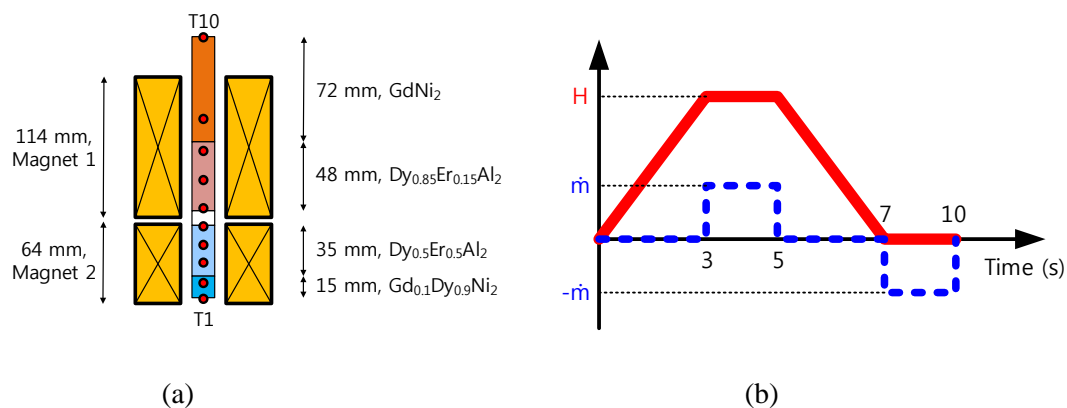


Figure 4. (a) Schematic of the multi-layered AMR and (b) the mass flow rate and the magnetic field variation during 1 cycle (10 s).

filled in AMR1 which cover the high temperature region, and Gd_{0.1}Dy_{0.9}Ni₂, Dy_{0.5}Er_{0.5}Al₂ are filled in AMR2 which operate at the low temperature part. Figure 4(a) illustrates the AMR assembly and the location of ten calibrated temperature sensors (Cernox, Lakeshore) in the AMR. Because the magnetic refrigerants of the AMR2 have smaller heat capacity than those of the AMR1, the bypass line between the AMR1 and the AMR2 is installed to adjust the helium flow rate for AMR2.

The LTS magnet magnetizes the experimental AMR system. The magnet consists of insulated multi-filamentary NbTi wire which is wound on a 1 inch diameter glass fiber reinforced plastic (GFRP, G-10). The current of the LTS magnet is controlled by a four-quadrant bipolar power supply (Model 642, Lakeshore). The LTS magnet can generate maximum 4 T with 70 A. The more detailed information of the AMR and the LTS magnet can be found in the previous literature [16].

3. Experimental results

3.1. Experimental procedure and operating conditions

The experimental procedure of the AMR system is as follows:

- 1) Filling liquid nitrogen in liquid nitrogen chamber
- 2) Pre-cooling of the AMR with liquid nitrogen by one way-circulating flow of the helium gas
- 3) Pre-cooling of the LTS magnet with liquid nitrogen
- 4) Cool-down of the LTS magnet with liquid helium
- 5) Test operation of the LTS magnet
- 6) Synchronizing the phase of the mass flow rate and the AC operation of the LTS magnet
- 7) Changing the experimental conditions

The mass flow rate and the magnetic field variation during 1 cycle is illustrated in Fig. 4(b). Plus sign of the mass flow rate means up-flow from the cold end to the warm end. The operating frequency of the AMR system is 0.1 Hz. The ramping time of the magnetic field and the helium gas flow time during the constant magnetic field are 3 s and 2 s, respectively. The AMR system is tested by varying the mass flow rate from 0.07 g/s to 0.15 g/s at the AMR1 and from 0.03 g/s to 0.07 g/s at the AMR2.

3.2. Performance of the AMR system

The performance of the AMR system with the variation of the mass flow rate (case 1~ case 3) is

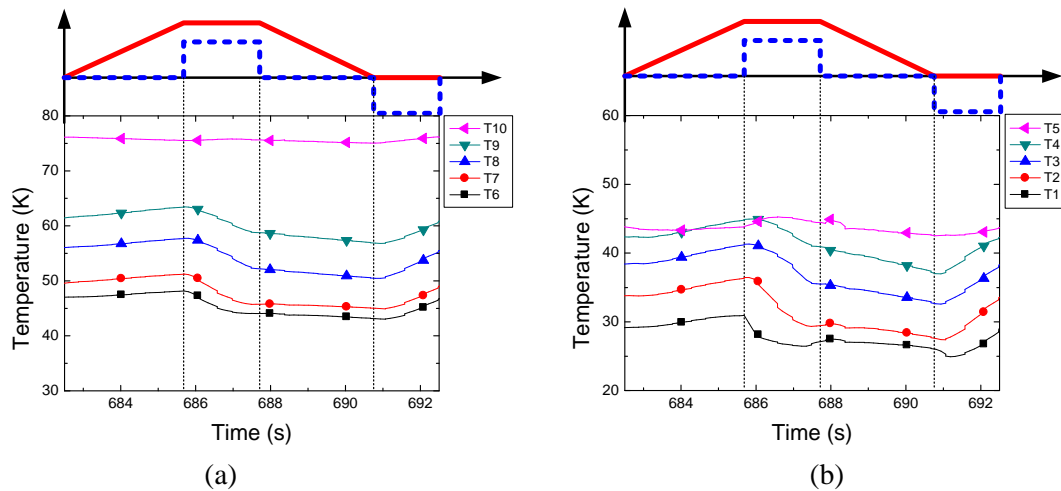


Figure 5. Case 1: internal temperature of (a) the AMR1 and (b) AMR2 with the mass flow rate of 0.15 g/s and 0.07 g/s, respectively at the cyclic steady state.

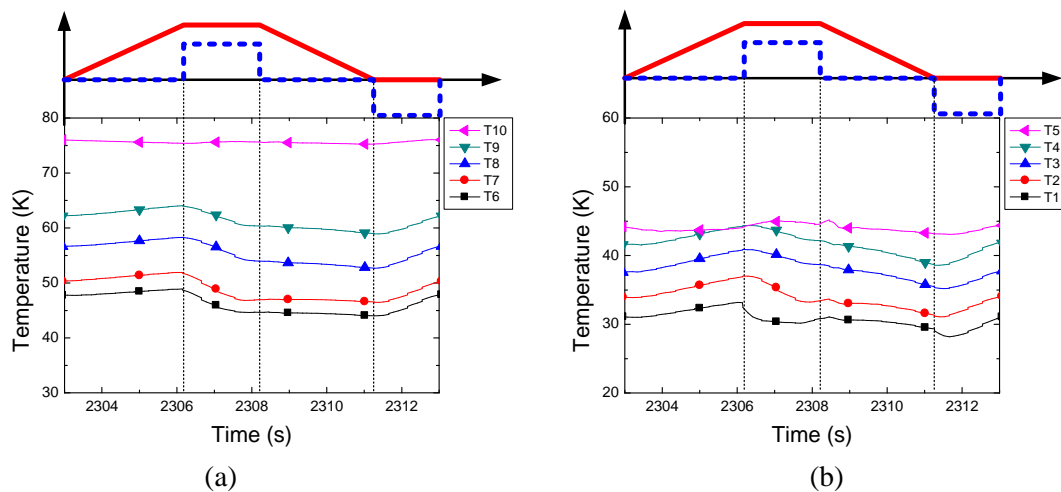


Figure 6. Case 2: internal temperature of (a) the AMR1 and (b) AMR2 with the mass flow rate of 0.12 g/s and 0.05 g/s, respectively at the cyclic steady state.

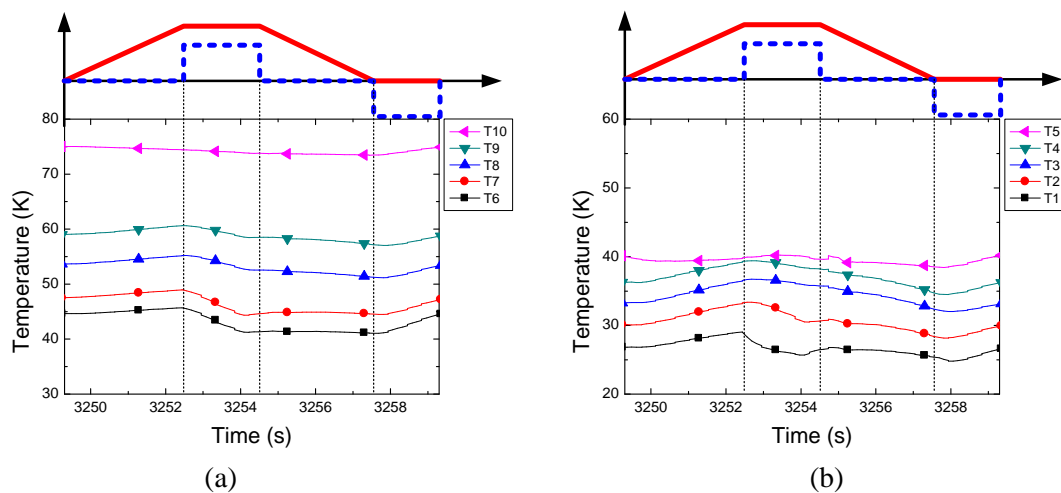


Figure 7. Case 3: Internal temperature of (a) the AMR1 and (b) AMR2 with the mass flow rate of 0.07 g/s and 0.03 g/s, respectively at the cyclic steady state.

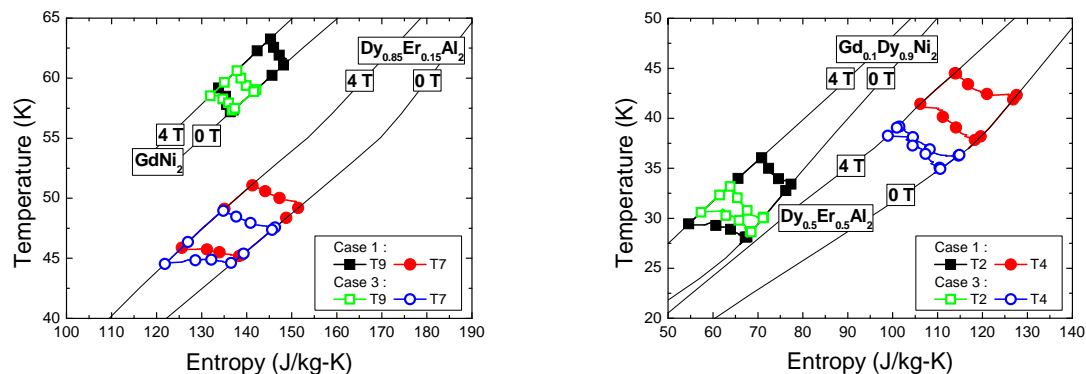


Figure 8. Temperature-entropy diagram of magnetic refrigerant in the AMR1 and the AMR2.

shown in Fig. 5 ~ Fig. 7. We can observe that the temperature of the AMR changes according to the variation of the magnetic field applied to the AMR. This means the cold end of the AMR is cooled by the magnetocaloric effect of the magnetic refrigerant. The temperature spans of the AMR1 and the AMR2 with the mass flow rate of case 1 are 34 K and 20 K, respectively. The lowest no-load temperature of the AMR2 is 25 K in case 1 and 3. However, the lowest temperature of the AMR2 in case 2 is higher than the others.

In order to observe the internal state of the magnetic refrigerants in the AMR, temperature-entropy diagrams for cyclic steady state are plotted in Fig. 8. Each position of the AMR has its own closed loop. The closed loops in case 1 has larger area than those in case 3. This means case 1 utilizes the magnetocaloric effect better than case 3. However, the lowest temperature is almost identical. In addition, areas of the closed loops in case 2 are about intermediate values between case 1 and case 3. It can be inferred that the lowest temperature of case 3 is mainly affected by the surrounding liquid helium. The radiation cooling by liquid helium which surrounds the AMR system with vacuum insulation does not seem to be negligible for small mass flow rate case. Since the AMR system in case 3 operates with the smallest mass flow rate, the heat leak due to the shuttle mass becomes negligible compared to helium gas effect. In contrast, the AMR system in case 1 operates with the largest mass flow rate. Therefore, the shuttle heat transfer by oscillating flow

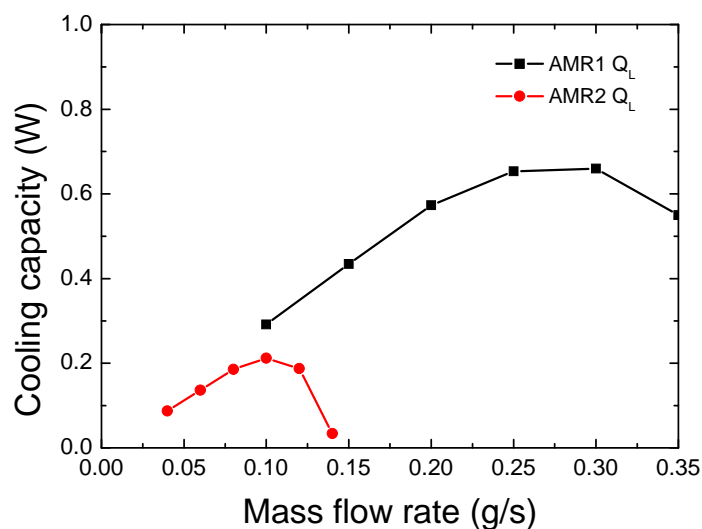


Figure 9. Cooling capacity of the AMR1 and AMR2 calculated by numerical simulation proposed by Park et al. [13]

negatively affects to the AMR performance more than that of case 3. Nevertheless, the better cooling performance shown in Fig. 8 enables the AMR in case 1 to reach lower temperature. This interpretation of the experimental results can be supported by numerical simulation results proposed by Park et al. [13]. Figure 9 presents the one dimensional numerical simulation results of the AMR system. The simulation results indicate the cooling capacity variation of the AMR1 and AMR2 with different mass flow rates. This simulation does not include shuttle heat transfer effect and liquid helium effect. The largest mass flow rates of the AMR1 and AMR2 in this paper are 0.15 g/s and 0.07 g/s, respectively. Therefore, according to the numerical results shown in Fig. 9, the cooling performance of the AMR system should increase with more mass flow rate in the experimental range. The experimental results of case 3 can be explained by the radiation cooling of liquid helium. The cooling capacity of case 3 must be small due to small helium mass flow rate. Since the detrimental shuttle heat transfer is negligible and liquid helium effect still exists, the AMRs tend to stay at lower temperature than other cases.

4. Conclusion

The two-stage AMRR system proposed for the operation between 77 K and 20 K has been tested. The modified AMR system reached the lowest no-load temperature of 25 K without gas expansion effect. However, the performance of the AMR is also influenced by shuttle heat transfer and the environmental liquid helium. Each effect of shuttle mass or liquid helium on the overall cooling performance has not been precisely decoupled from the original MCE. In order to investigate the cooling performance of the AMR system more accurately, two additional effects mentioned above have to be minimized.

5. Acknowledgments

This research was supported by the Converging Research Center Program through the Ministry of Science, ICT and Future Planning, Korea (2014M3C1A8048836).

6. References

- [1] Shirron P, Canavan E, DiPirro M, Francis J, Jackson M, Tuttle J, King T and Grabowski M 2004 *Cryogenics* **44** 581
- [2] Bartlett J, Hardy G, Hepburn I D, Brockley-Blatt C, Coker P, Crofts E, Winter B, Milward S, Stafford-Allen R, Brownhill M, Reed J, Linder M and Rando N 2010 *Cryogenics* **50** 582
- [3] Duband L, Duval J M, Luchier N and D'Escrivan S D 2011 *Cryocoolers* **16** 699
- [4] Jeong S 2014 *Cryogenics* **62** 193
- [5] Yu B, Liu M, Egolf P W and Kitanovski A 2010 *Int. J. Refrig.* **33** 1029
- [6] Tura A, Nielsen K K and Rowe A 2012 *Int. J. of Refrig.* **35**
- [7] Chiba Y, Smaïli A, Mahmed C, Balli M and Sari O 2014 *Int. J. of Refrig.* **37** 36
- [8] Arnold D S, Tura A, Ruebsaat-Trott A and Rowe A 2014 *Int. J. of Refrig.* **37** 99
- [9] Bahl C R H, Engelbrecht K, Eriksen D, Lozano J A, Bjørk R, Geyti J, Nielsen K K, Smith A and Pryds N 2013 *Int. J. of Refrig.* **37** 78
- [10] Zhang L, Sherif S A, Veziroglu T N and Sheffield J W 1992 *Cryogenics* **33** 667
- [11] Zhang L, Sherif S A, DeGregoria A J, Zimm C B and Veziroglu T N 2000 *Cryogenics* **40** 269
- [12] Matsumoto K, Kondo T, Ikeda Masakazu and Numazawa T 2011 *Cryogenics* **51** 353
- [13] Park I, Kim Y, Park J and Jeong S 2015 *Cryogenics* **70** 57
- [14] Numazawa T, Kamiya K, Utaki T and Matsumoto K 2014 *Cryogenics* **62** 185
- [15] Hirayama Y, Okada H, Nakagawa T, Yamamoto T, Kusunose T, Numazawa T, Mastumoto K, Irie T and Nakamura E 2011 *Cryocoolers* **16** 531
- [16] Kim Y, Park I and Jeong S 2013 *Cryogenics* **57** 113